BIOCHEMISTRY
including biophysical chemistry & molecular biology

Article

pubs.acs.org/biochemistry

Involvement of Phenylalanine 297 in the Construction of the Substrate Pocket of Human Aminopeptidase B

Atsushi Ohnishi,*[,†] Jobu Watanabe,[†] Yuko Ogawa,[†] Yoshikuni Goto,[†] Akira Hattori,[‡] and Masafumi Tsujimoto[†]

[†]Faculty of Pharmaceutical Sciences, Teikyo Heisei University, Nakano, Tokyo 164-8530, Japan

[‡]Department of System Chemotherapy and Molecular Sciences, Graduate School of Pharmaceutical Sciences, Kyoto University, Kyoto 606-8501, Japan

ABSTRACT: Aminopeptidase B (APB, EC 3.4.11.6) preferentially hydrolyzes the N-terminal basic amino acids of synthetic and peptide substrates and requires a physiological concentration of NaCl for optimal activity. In this study, we used site-directed mutagenesis and molecular modeling to search for an amino acid residue that is critical for the enzymatic properties of human APB. Substitution of Phe297 with Tyr caused a significant decrease in hydrolytic activity toward synthetic and peptide substrates as well as chloride anion sensitivity. Molecular modeling suggests that Phe297 contributes to the construction of the substrate pocket of APB, which is wide enough to hold a chloride anion and allow the interaction of Gln169 with the N-terminal Arg residue of the substrate through bridging with the chloride anion. These results indicate that Phe297 is crucial for the optimal enzymatic activity and chloride anion sensitivity of APB via formation of the optimal structure of the catalytic pocket.

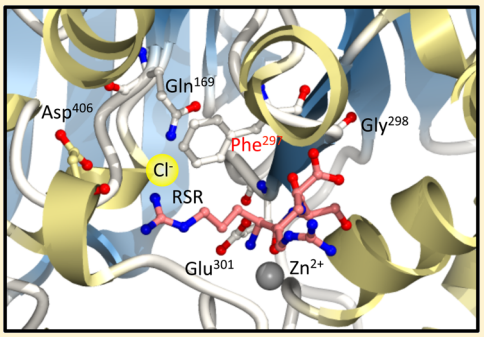

Aminopeptidase B (APB, EC 3.4.11.6), first detected in several rat tissues, is a soluble monomeric protein that preferentially releases basic amino acids (Arg and Lys) from the N-terminus of several peptide and fluorogenic substrates.[1] Characterization of the enzymatic properties of APB revealed that the hydrolytic activity of the enzyme is enhanced in the presence of physiological concentrations of chloride anions.[2] APB belongs to the M1 family of zinc aminopeptidases that contain $HEXXH(X)_{18}E$ and GXMEN motifs essential for enzymatic activity.[3,4]

Because of its preference for basic amino acids, APB was suggested to be involved in the proteolytic processing and maturation of peptide hormones and neurotransmitters.[1] It was reported that APB is involved in the generation of active peptides through cleavage of extended N-terminal Arg and Lys residues in intermediate propeptides produced by endopeptidases such as cathepsin L and *N*-arginine dibasic convertase (NRD)/nardilysin.[5−7] Given that the APB hydrolytic activity toward Arg and Lys residues is essential for processing and maturation of hormones and neurotransmitters, it is important to elucidate the structural aspects underlying APB activity.

Site-directed mutagenesis and molecular modeling are useful techniques for elucidating the structural and functional features of APB in the absence of a crystal structure. Using site-directed mutagenesis, the roles of amino acid residues comprising the $HEXXH(X)_{18}E$ and GXMEN motifs of APB were elucidated.[8,9] Moreover, the roles of Tyr residues distributed throughout the APB molecule were comprehensively analyzed.[10] It was reported that replacement of Asp405 with Ala or Asn in rat APB caused a change in substrate specificity toward fluorogenic substrates.[11] We also reported that Gln169 of human APB is critical for the optimal enzymatic activity and chloride anion sensitivity.[12]

In this study, we extended our search for an amino acid residue responsible for the enzymatic properties of human APB. We found that Phe297 is critical for the optimal enzymatic activity and chloride anion sensitivity of this enzyme. Additionally, molecular modeling suggests that Phe297 contributes to the formation and maintenance of the optimal structure of the substrate pocket and thus plays a key role in the distinct enzymatic properties of the enzyme.

EXPERIMENTAL PROCEDURES

Site-Directed Mutagenesis. A DNA sequence encoding F297Y and F297A APB was generated by polymerase chain reaction (PCR) using the full-length human APB cDNA (RIKEN clone ID IRAL002L13) as the template. PCRs were conducted in 0.2 mL microcentrifuge tubes with a 30 μL reaction volume and performed with the following program: 95 °C for 4 min, followed by 20 cycles at 95 °C for 1 min, 55 °C for 1 min, and 68 °C for 18 min, using Pyrobest DNA polymerase (Takara, Kyoto, Japan). The sense primer A (5′-TAGAGGATCCATGGCGAGCGGCGAGCATT-3′), containing a *Bam*HI sequence for directional cloning and an initiation ATG codon (underlined), and the antisense primer complementary to the desired sequence were used for the amplification of the upstream fragments. The downstream

Received: April 2, 2015
Published: September 9, 2015

DOI: 10.1021/acs.biochem.5b00964
Biochemistry 2015, 54, 6062−6070

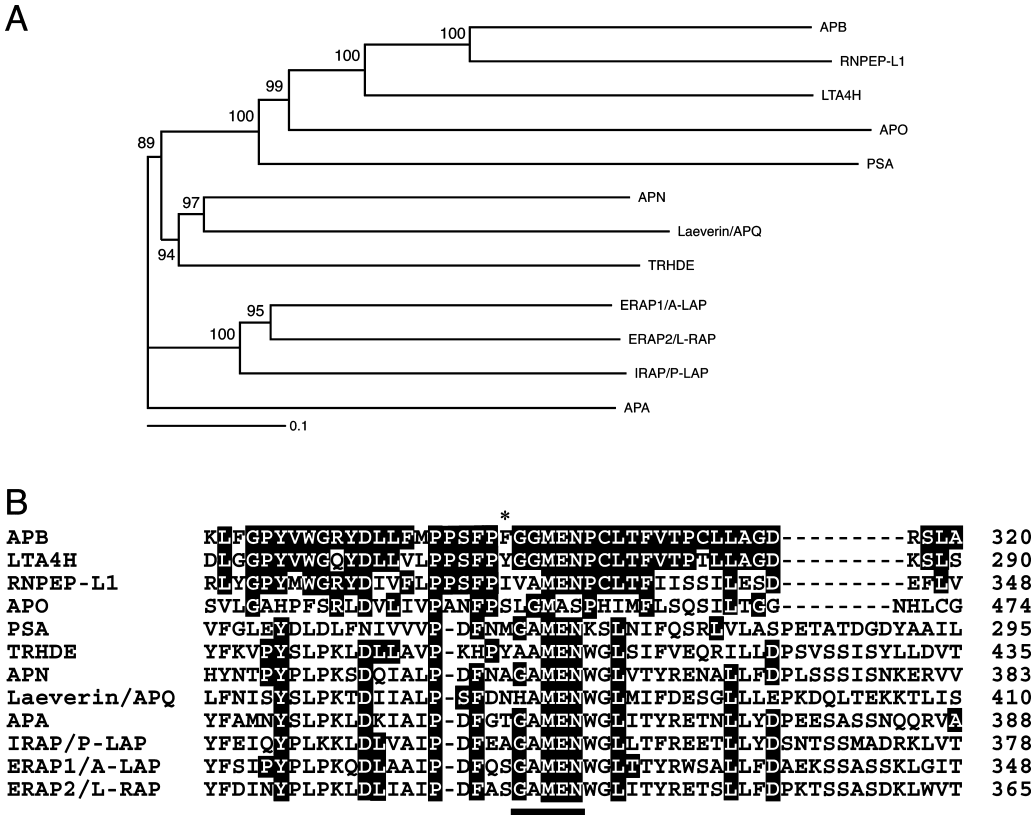

Figure 1. Identification of an amino acid residue characteristic of human APB. (A) Phylogenetic analysis of the human aminopeptidases belonging to the M1 family. Analysis was performed using the maximum likelihood method in MEGA version 6.0 following sequence alignment in ClustalW and was tested by 1000 bootstrap replicates. The sequence data used for the analysis are as follows: APB (aminopeptidase B, NM_020216), RNPEP-L1 (arginyl aminopeptidase-like 1, NM_018226), LTA4H (leukotriene A_4 hydrolase, NM_000895), APO (aminopeptidase O, NM_001193329), PSA (puromycin-sensitive aminopeptidase, NM_006310), APN (aminopeptidase N, NM_001150), laeverin/APQ (laeverin/aminopeptidase Q, NM_173800), TRHDE (thyrotropin-releasing hormone-degrading enzyme, NM_013381), ERAP1/A-LAP (endoplasmic reticulum aminopeptidase-1/adipocyte-derived leucine aminopeptidase, NM_001040458), ERAP2/L-RAP (endoplasmic reticulum aminopeptidase-2/leukocyte-derived aminopeptidase, NM_022350), IRAP/P-LAP (insulin-regulated aminopeptidase/placental leucine aminopeptidase, NM_005575), and APA (aminopeptidase A, NM_001977). (B) Alignment around the GXMEN motif of human APB with other human members of the M1 family of aminopeptidases. Gaps were inserted into the sequence to obtain the optimal alignments. Residues identical with those of APB are highlighted in black. An asterisk indicates the residues on which this study focused. The underline indicates the position of the GXMEN motif.

fragment was amplified using mutagenic sense primers and primer B (5′-TGAGTCGACCTAACTGCCCTTGGGT-3′) containing the *Sal*I sequence.

The two products of these reactions were used as templates for the second round of PCR. Secondary PCR was conducted with primers A and B as follows: 95 °C for 4 min, followed by 20 cycles at 95 °C for 1 min, 55 °C for 1 min, and 68 °C for 18 min. The resultant products were inserted into expression vector pQE-30 (Qiagen, Valencia, CA) using the TOPO cloning system (Invitrogen, La Jolla, CA).

The point mutations of the APB constructs were generated by site-directed mutagenesis using the KOD-Plus-Mutagenesis Kit (Toyobo, Osaka, Japan) according to the manufacturer's instructions. Specific oligonucleotide primer pairs [for F297Y, sense primer (5′-TACGGAGGAGATGGAGAACCCTTGTC-3′) and antisense primer (5′-TGGAAAGGACGGTGGCATG-AAGAGCA-3′); for F297A, sense primer (5′-GCAGGAGGA-GATGGAGAACCCTTGTC-3′) and antisense primer (5′-TGGAAAGGACGGTGGCATGAAGAGCA-3′); nucleotide sequences corresponding to Phe297 are underlined] were designed on the basis of their published sequence.

The DNA sequences of the products were confirmed using a 3000 Genetic Analyzer (Life Technologies, Carlsbad, CA).

Expression and Purification of the Wild-Type, F297Y, and F297A APBs. The resultant plasmids were transformed into *Escherichia coli* JM109 to produce recombinant proteins. For expression of the recombinant human APB or its mutants fused to an N-terminal His_6 affinity tag, bacteria were cultured until the OD_{600} reached 0.5−0.7. To induce synthesis of the recombinant proteins, IPTG was added to the cultures to a final concentration of 0.2 mM. Cells were cultured for 24 h at 20 °C in 1 L of LB broth containing 100 μg/mL ampicillin.

To purify the recombinant proteins, bacteria were collected by centrifugation at 4000*g* for 30 min and sonicated on ice five times for 30 s using a sonicator (model 250D sonifier, Branson, Danbury, CT). Soluble proteins were recovered after centrifugation at 10000*g*, and the supernatants were applied to a DEAE Toyopearl column (Tosoh, Tokyo, Japan) equilibrated in 25 mM Tris-HCl buffer (pH 7.5) and eluted with 25 mM Tris-HCl buffer (pH 7.5) containing 50 mM NaCl. The eluates were applied to a TALON column (Clontech, Palo Alto, CA) and eluted with 150 mM imidazole. The active fractions were collected, concentrated, and subjected to further characterization.

For sodium dodecyl sulfate−polyacrylamide gel electrophoresis (SDS−PAGE), 1 μg of recombinant protein was

DOI: 10.1021/acs.biochem.5b00964
Biochemistry 2015, 54, 6062−6070

incubated with 80 mM Tris-HCl buffer (pH 8.8) containing 1% SDS and 2.5% 2-mercaptoethanol at 95 °C for 5 min and then developed.

Measurement of APB Aminopeptidase Activity. The aminopeptidase activity of the human APB and its mutants was determined using the fluorogenic substrates, aminoacyl-4-methylcoumaryl-7-amides (aminoacyl-MCAs). The reaction mixture containing various concentrations of amino-acyl-MCA and the enzyme (0.1 μg/mL) in 50 μL of 20 mM Tris-HCl buffer (pH 7.4) with 150 mM NaCl was incubated at 37 °C for 15 min. The amount of released 7-amino-4-methylcoumarin was measured by spectrofluorophotometry (MTP-810Lab, Hitachi, Tokyo, Japan) at an excitation wavelength of 380 nm and an emission wavelength of 460 nm. The kinetic parameters were calculated by Lineweaver–Burk plots. The results are represented as K_m, k_{cat}, and k_{cat}/K_m values. All measurements were performed in triplicate.

Effect of NaCl and Inhibitors on APB Aminopeptidase Activity. To confirm the effect of NaCl on the aminopeptidase activity, the recombinant proteins (0.1 μg/mL) and 25 μM Arg-MCA were mixed in 0.2 M borate buffer (pH 7.4) containing various concentrations of NaCl. After incubation, the amount of released 7-amino-4-methylcoumarin was measured as described above.

To evaluate the inhibitory effects of bestatin, arphamenine A, and arphamenine B, recombinant proteins (0.1 μg/mL) were mixed with various concentrations of inhibitors in 50 μL of 20 mM Tris-HCl buffer (pH 7.4) containing 150 mM NaCl on ice for 5 min and then incubated with 25 μM Arg-MCA at 37 °C for 15 min, and the amount of released 7-amino-4-methylcoumarine was measured as described above.

Cleavage of Peptide Substrates by the Wild-Type and F297Y APBs. Peptide substrates (25 μM; Peptide Institute, Osaka, Japan) were incubated with the recombinant enzymes (4 μg/mL) at 37 °C for 4 h in 20 mM Tris-HCl buffer (pH 7.4) containing 150 mM NaCl. The reaction was terminated by addition of 2.5% (v/v) formic acid. The reaction products were separated on a reversed phase column, COSMOSIL $5C_{18}$-AR-300 (4.6 mm inner diameter × 250 mm; Nacalai Tesque, Kyoto, Japan), using an automated HPLC system (LC-2010AHT; Shimadzu, Kyoto, Japan). After incubation with the APBs, peptide fragments were isocratically eluted at a flow rate of 0.5 mL/min with 19% acetonitrile containing 0.086% trifluoroacetic acid. All measurements were performed in triplicate.

Molecular Modeling of the Human APB. The published X-ray crystallographic structure of the human LTA4H with an RSR-containing substrate (3B7S) was used as a template for modeling the catalytic site of the human APB using the SWISS-MODEL Internet server. To optimize the structure, hydrogen atoms were added to the initial model and the protonation states were assigned using the Protonate-3D tool within the MOE2012.10 software package (Chemical Computing Group, Montreal, QC). Energy minimization was conducted using the AMBER12:EHT force field. For docking calculations, the backbones of the model were fixed and the side-chain conformations were then subjected to another refinement procedure, including several rounds of energy minimization (until convergence) using the Molecular Mechanics method. The structures were represented using the CueMol program (R. Ishitani, CueMol: Molecular Visualization Framework).

Materials. Asp-, Gln-, Glu-, Ile-, Tyr-, Val-, and *S*-benzyl-Cys-MCAs were purchased from Bachem AG (Bubendorf, Switzerland). Ala-, Arg-, Leu-, Lys-, Met-, and Phe-MCAs were from the Peptide Institute. Bestatin, arphamenine A, and arphamenine B were also obtained from the Peptide Institute. [Arg^0]-Met-enkephalin was purchased from Phoenix Peptides (Belmont, CA). Kallidin was obtained from the Peptide Institute.

RESULTS

Identification of an Amino Acid Residue Responsible for the Characteristic Features of APB. Figure 1A shows a phylogenetic tree of the M1 family of human aminopeptidases based on their amino acid sequence identities. Twelve proteins belonging to the family have been identified in the human genome, and their enzymatic properties have been characterized.[4,13−17] It seems that APB, LTA4H, and RNPEP-L1 (arginyl aminopeptidase-like 1) comprise a distinct subfamily together with APO and PSA.[4,15,16] To identify whether there was a single residue responsible for the unique characteristics and enzymatic activity of APB, we compared the amino acid sequences of M1 aminopeptidases around the GXMEN motif (Figure 1B). As expected, alignment of M1 aminopeptidases around this motif indicated that APB has a sequence highly identical with those of LTA4H and RNPEP-L1, whereas it is less similar to other M1 aminopeptidases. Intriguingly, the GXMEN motif-containing sequences, Pro292−Pro310 of APB and Pro262−Pro280 of LTA4H, are identical except for Phe297 and Tyr267, respectively. As both residues are located just adjacent to the N-terminal side of the GXMEN motif, we speculated that Phe297 may be important for the characteristic features of APB. Our previous molecular modeling suggested that the substrate pocket of APB is wide enough to hold a chloride anion, whereas that of LTA4H is too narrow to retain an anion.[12] We hypothesized that Phe297 plays a role in the formation of the appropriate structure of the catalytic pocket and contributes to the characteristic properties of APB.

To elucidate the role of Phe297, the wild-type, F297Y, and F297A APBs were expressed in *E. coli* and purified to homogeneity via SDS−PAGE (Figure 2). All the enzymes showed single bands on SDS−PAGE with apparent molecular masses of ∼74 kDa. We used these preparations to measure the activity of the enzymes.

Enzymatic Activity of the Wild-Type and Mutant APBs toward Synthetic Substrates. Figure 3 shows the enzymatic activity of the wild-type and mutant APBs toward various synthetic substrates measured in the presence or absence of chloride anions. When measured in the presence of chloride anions, the wild-type APB preferentially cleaved the Arg-MCA, followed by Lys-MCA, showing an apparent preference for the basic amino acids of the enzyme, as described previously.[12] The enzymatic activity of F297Y APB measured in the presence of chloride anions was significantly lower, and only <10% activity was observed toward the most efficient substrate, Arg-MCA. The kinetic parameters of the wild-type and F297Y APBs toward Arg-MCA and Lys-MCA measured in the presence of chloride anions revealed that the catalytic efficiency (k_{cat}/K_m) of F297Y APB was ∼13- and ∼15-fold, respectively, lower than that of the wild-type enzyme (Table 1). This observation was a result of both an increase in K_m and a decrease in k_{cat}. In the absence of chloride anions, both enzymes showed significantly lower activities toward the synthetic substrates compared with the activity of the wild-type enzyme measured in the presence of chloride anions. These results indicate that replacement of Phe297 with Tyr caused the reduction of enzymatic activity of

DOI: 10.1021/acs.biochem.5b00964
Biochemistry 2015, 54, 6062−6070

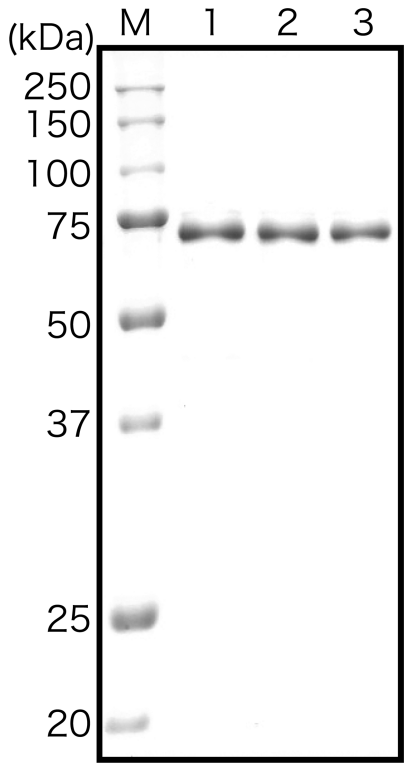

Figure 2. SDS−PAGE analyses of recombinant APBs. Three recombinant proteins were subjected to SDS−PAGE in 12% acrylamide gels and stained with Coomassie brilliant blue R-250: lane 1, marker proteins; lane 2, wild-type APB; lane 3, F297Y APB; lane 4, F297A APB.

APB toward synthetic substrates. Very small differences were observed between the wild-type and F297Y mutant APBs in terms of their substrate specificities. We also measured the enzymatic activity of the F297A mutant APB and found only negligible activity toward all substrates tested.

We next compared the effects of aminopeptidase inhibitors on hydrolytic activities of the wild-type and F297Y mutant APBs toward the Arg-MCA substrate (Table 2). Upon measurement in the presence of 150 mM NaCl, it was apparent that bestatin (Phe-Leu analogue), arphamenine A (Arg-Phe analogue), and arphamenine B (Arg-Tyr analogue), which interact with the substrate pocket of APB, all inhibited the wild-type enzyme more efficiently than the mutant. These results suggest that Phe297 is critical to the optimal enzymatic activity of APB by affecting the substrate pocket structure.

Effects of NaCl on the Enzymatic Activity of the Wild-Type and Mutant APBs toward Synthetic Substrates. Because both the wild-type and F297Y APBs still retained measurable activities toward Arg-MCA in the absence of chloride anions, we compared the effects of NaCl on the activity of the enzymes (Figure 4). As shown previously,[12] at a physiological concentration of NaCl (150 mM), an ∼5-fold increase in the enzymatic activity of the wild-type enzyme was observed compared with the activity measured in the presence of 10 mM NaCl, and the calculated EC_{50} value was 37.7 ± 12.1 mM. F297Y APB showed only a small amount of activity in 10 mM NaCl. However, an increase in activity was clearly observed at 150 mM NaCl, and the calculated EC_{50} value was 182 ± 58.4 mM. Because the EC_{50} values reflect the binding affinity of chloride anions for the enzymes, replacement of Phe297 with Tyr may cause a structural modification in the catalytic pocket, altering the enzymatic properties of APB.

Enzymatic Activity of the Wild-Type and Mutant APBs toward Peptide Substrates. We next compared the cleavage of several peptide substrates by the wild-type and F297Y APBs. Figure 5A shows the cleavage of [Arg^0]-Met-enkephalin (RYGGFM), one of the most effective substrates of APB,[1] by APBs. As reported previously,[12] generation and subsequent degradation of Met-enkephalin by the wild-type enzyme were clearly observed, and 68% of [Arg^0]-Met-enkephalin was degraded into Met-enkephalin and de-[Tyr]-Met-enkephalin after incubation for 4 h. Cleavage of [Arg^0]-Met-enkephalin by F297Y APB was not detectable over the same incubation time. We also examined the cleavage of kallidin (KRPPGFSPFR) by the wild-type and mutant APBs. While 73% of kallidin was converted into bradykinin by the wild-type enzyme during the 4 h incubation, F297Y APB had no detectable activity toward kallidin (Figure 5B). We also tested the activity of F297A APB and found that it did not cleave [Arg^0]-Met-enkephalin and kallidin (data not shown). These results indicate that similar to what was observed for the synthetic substrates, F297Y and F297A APBs were significantly less active than wild-type APB, even toward more favorable peptide substrates.

Figure 5C shows the effect of chloride anion on the APB-mediated cleavage of [Arg^0]-Met-enkephalin. While in the presence of 150 mM NaCl, 68% cleavage was observed within 4 h, the wild-type APB cleaved 7% [Arg^0]-Met-enkephalin in the absence of NaCl, indicating that as in the case of synthetic substrates, APB-mediated cleavage of peptide substrates was also affected by chloride anion. We also examined the effect of chloride anion on the cleavage of kallidin and found that the anion was required for maximal cleavage (data not shown). Thus, Phe297 affects enzymatic activity and chloride anion sensitivity toward both synthetic fluorogenic and peptide substrates.

Molecular Modeling of the Wild-Type and Mutant APBs. We next compared the substrate pocket structures of the wild-type and F297Y APBs by molecular modeling. Figure 6 shows the surface modeling of the substrate pocket structure of the wild-type and F297Y APBs coupled with the putative substrate RSR with reference to the role of Phe297 in the spatial relationship between Gln169 (or corresponding residues) of the enzyme and RSR. For comparison, we also modeled the substrate pocket of LTA4H for which a crystal structure is available (Figure 6A).[18] The substrate pocket of LTA4H is relatively narrow as shown previously.[12] Tyr267, which corresponds to Phe297 of the wild-type APB, seems to block the interaction between Arg1 of RSR and Gln134. Chloride anion bridging seems unlikely, because of the inappropriate orientation of Arg1 of RSR relative to Gln134 in the pocket. When the substrate pocket of the wild-type APB was modeled, it seemed plausible that Phe297 allows the formation of a broad space for holding a chloride anion (Figure 6B). The positive electric potential provided by Gln169 makes it possible for a chloride anion to bridge the interaction between Gln169 and Arg1 of RSR. In the absence of a chloride anion, it seems likely that although oriented properly, Arg1 of RSR cannot interact with Gln169 directly because of the long distance between them.[12] Like LTA4H, the substrate pocket of F297Y APB is rather narrow and the hydroxyl group of Tyr297 may restrict the formation of a chloride anion-mediated interaction between Gln169 and Arg1 of RSR. Additionally, Arg1 of RSR is inappropriately oriented in the substrate pocket

DOI: 10.1021/acs.biochem.5b00964
Biochemistry 2015, 54, 6062−6070

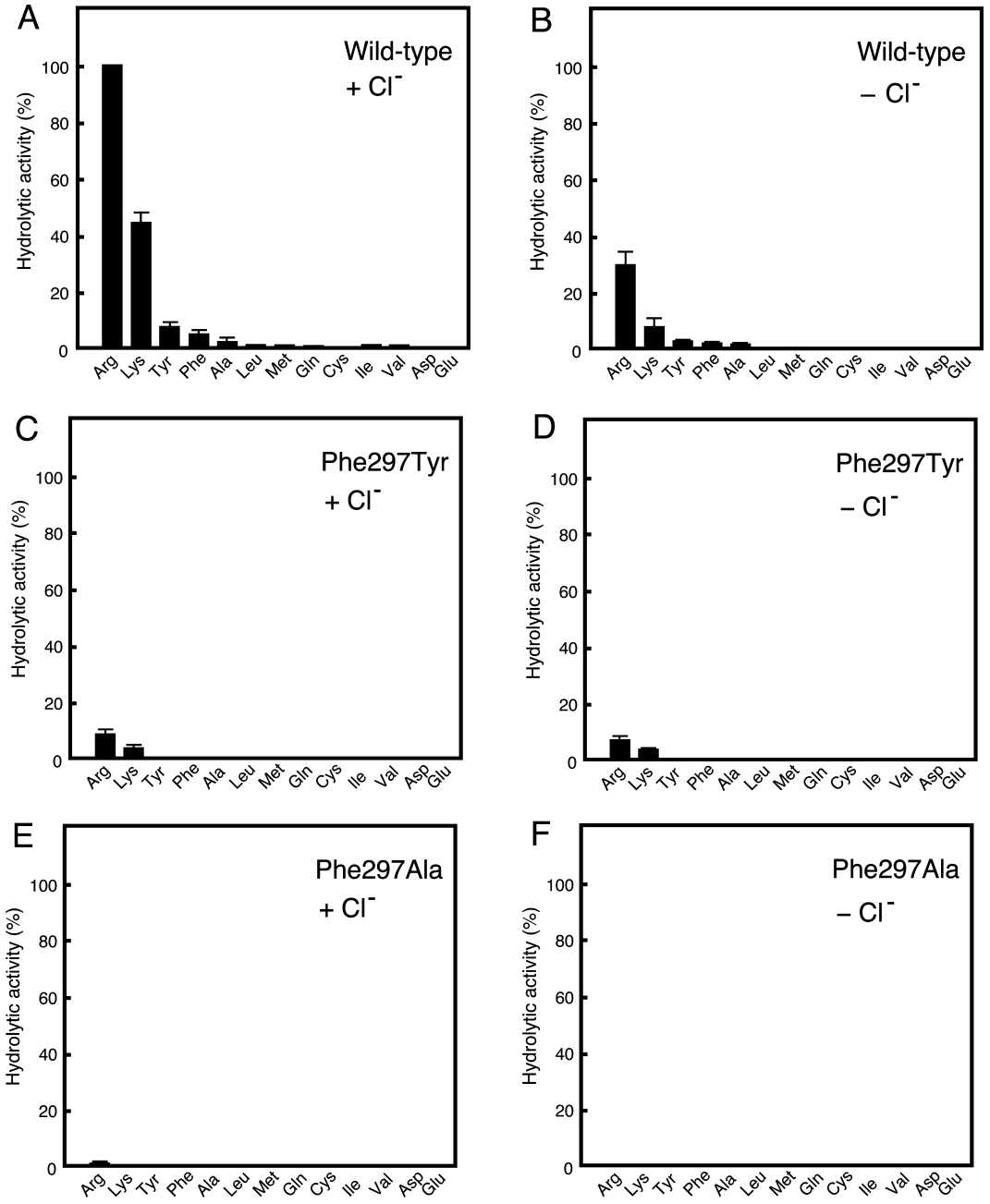

Figure 3. Enzymatic activity of the wild-type, F297Y, and F297A APBs toward synthetic fluorogenic substrates. Purified enzymes (0.1 μg/mL) were incubated with 100 μM MCA substrates at 37 °C for 15 min in the presence or absence of NaCl (150 mM). Hydrolytic activities are expressed relative to the wild-type enzyme activity (100%) toward Arg-MCA. Each bar represents the mean ± SD (n = 3).

Table 1. Kinetic Parameters[a] of Wild-Type and Phe297Tyr APBs toward Arg-MCA and Lys-MCA

substrate	enzyme	K_m (μM)	k_{cat} (s^{-1})	k_{cat}/K_m ($\times 10^{-3}$ μM^{-1} s^{-1})
Arg-MCA	wild-type	52.9 ± 4.4	9.64 ± 1.03	182 ± 2.3
	Phe297Tyr	208 ± 11	2.95 ± 0.69	14.2 ± 6.2
Lys-MCA	wild-type	323 ± 10	12.9 ± 1.15	39.9 ± 3.3
	Phe297Tyr	598 ± 13	1.56 ± 0.09	2.61 ± 0.5

[a]Kinetic parameters were determined from Lineweaver–Burk plots. Reactions were performed at 37 °C for 15 min with 150 mM NaCl. The substrates were reacted at different concentrations (1, 2, 5, 10, 20, and 50 μM). The values shown are means ± SD (n = 3).

Table 2. IC_{50} Values of the Inhibitors toward Wild-Type and Phe297Tyr APBs[a]

APB	bestatin (nM)	arphamenine A (nM)	arphamenine B (nM)
wild-type	3.82 ± 0.49	4.02 ± 0.58	0.70 ± 0.10
Phe297Tyr	352 ± 61	27.5 ± 5.3	1.87 ± 0.63

[a]Purified enzymes (0.1 μg/mL) were incubated with 25 μM Arg-MCA substrates with three aminopeptidase inhibitors in the presence of 150 mM NaCl. The hydrolytic activity toward Arg-MCA measured in the absence of an inhibitor was taken to be 100%. The values representing IC_{50} values are means ± SD (n = 3).

relative to Gln169 and is unable to interact with Gln169. Thus, it is plausible that Phe297 but not Tyr can support the interaction between Gln169 and the side chain of the N-

DOI: 10.1021/acs.biochem.5b00964
Biochemistry 2015, 54, 6062–6070

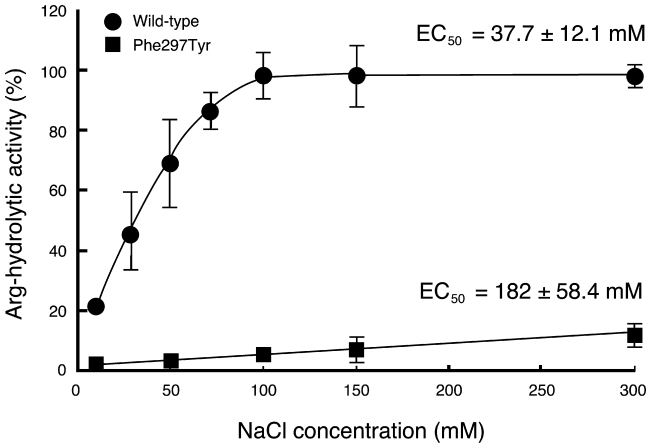

Figure 4. Effects of the NaCl concentration on the enzymatic activity of the wild-type and F297Y APBs. Hydrolytic activities are expressed relative to the wild-type enzyme activity (100%) measured in the presence of 300 mM NaCl. Each point represents the mean ± SD (n = 3).

terminal amino acid of the substrate via chloride anion bridging. We also estimated the substrate pocket of RSR-coupled RNPEP-L1 (Figure 6D). It was reported that RNPEP-L1 showed a chloride anion-independent aminopeptidase activity with a preference for Met and Gln but not for Arg.[16] Modeling of the substrate pocket suggests that Ile325 does not restrict the interaction of Gln196 and Arg1 of RSR. It is wide enough to allow the flexible interaction of Gln196 with Arg1 of RSR. Considering that the distance between Gln169 of APB and Arg1 of RSR (4.41 Å) is longer than that between Gln196 of RNPEP-L1 and Arg1 of RSR (3.86 Å), it is conceivable that Gln196 of RNPEP-L1 may interact with an appropriate substrate peptide without chloride anion bridging. Taken together, via comparison of the substrate pockets of several aminopeptidases, it is plausible that Phe297 of the wild-type APB plays important roles in the construction of the proper substrate pocket, which allows a chloride anion-mediated interaction of Gln169 with the N-terminal basic amino acids of substrate peptides.

DISCUSSION

In terms of aminopeptidases, APB is unique in its preference for basic amino acids and its sensitivity toward chloride anion.[1] In this study, the roles of Phe297 in the enzymatic properties of human APB were examined. We found that replacement of Phe297 with Tyr caused a significant decrease in hydrolytic activity toward both synthetic fluorogenic and peptide substrates. Decreased sensitivities to several APB inhibitors were also seen. Additionally, substitution of Phe297 with Tyr was found to attenuate the chloride anion sensitivity of the enzyme. These results suggest that Phe297 is critical for the enzymatic properties of APB by affecting its substrate pocket structure.

According to our molecular modeling, the substrate pocket of the wild-type but not F297Y APB is wide enough to hold a chloride anion. Thus, it is plausible that Phe297 assists the interaction of Gln169, a residue responsible for the enzymatic activity and substrate specificity of APB, with the N-terminal basic amino acids of the peptide substrates via formation of a chloride anion bridge. Because of the broad substrate pocket of the wild-type APB, the N-terminal basic amino acids of the

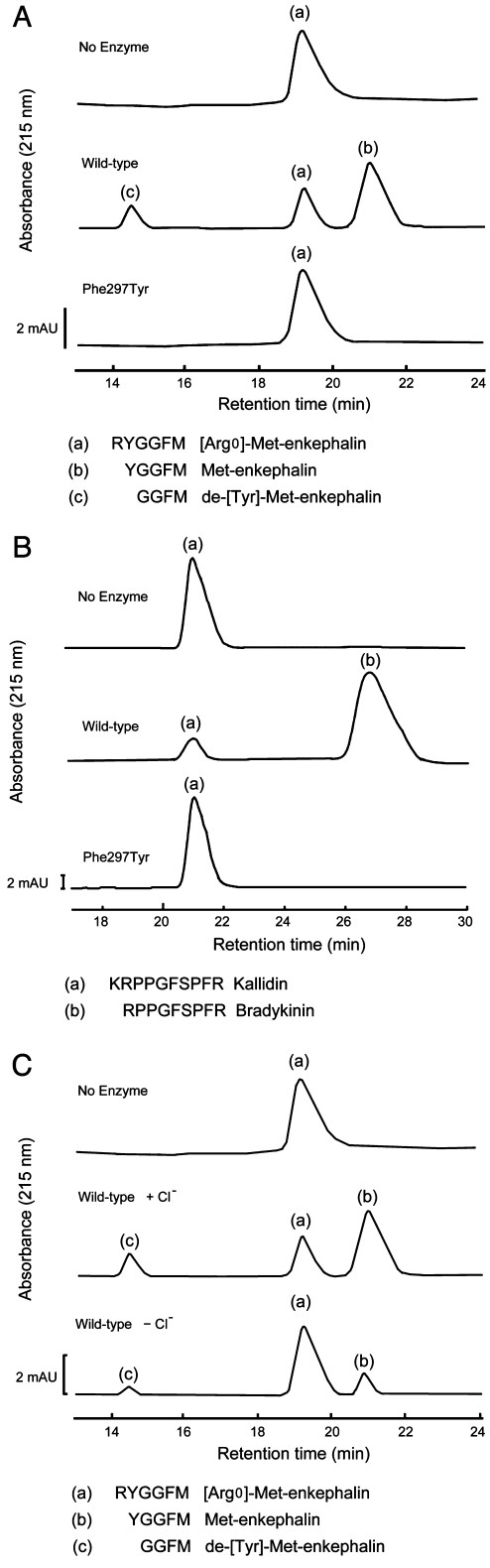

Figure 5. Cleavage of [Arg^0]-Met-enkephalin and kallidin by the wild-type and F297Y APBs. [Arg^0]-Met-enkephalin (25 μM) (A) and kallidin (25 μM) (B) were incubated with the purified enzymes (4 μg/mL) at 37 °C for 4 h. (C) Effect of chloride anion on the cleavage of [Arg^0]-Met-enkephalin by the wild-type APB. [Arg^0]-Met-enkephalin (25 μM) was incubated with the wild-type APB in the presence or absence of 150 mM NaCl at 37 °C for 4 h. The generated peptides were separated by HPLC. mAU, milli-absorbance units.

DOI: 10.1021/acs.biochem.5b00964
Biochemistry 2015, 54, 6062−6070

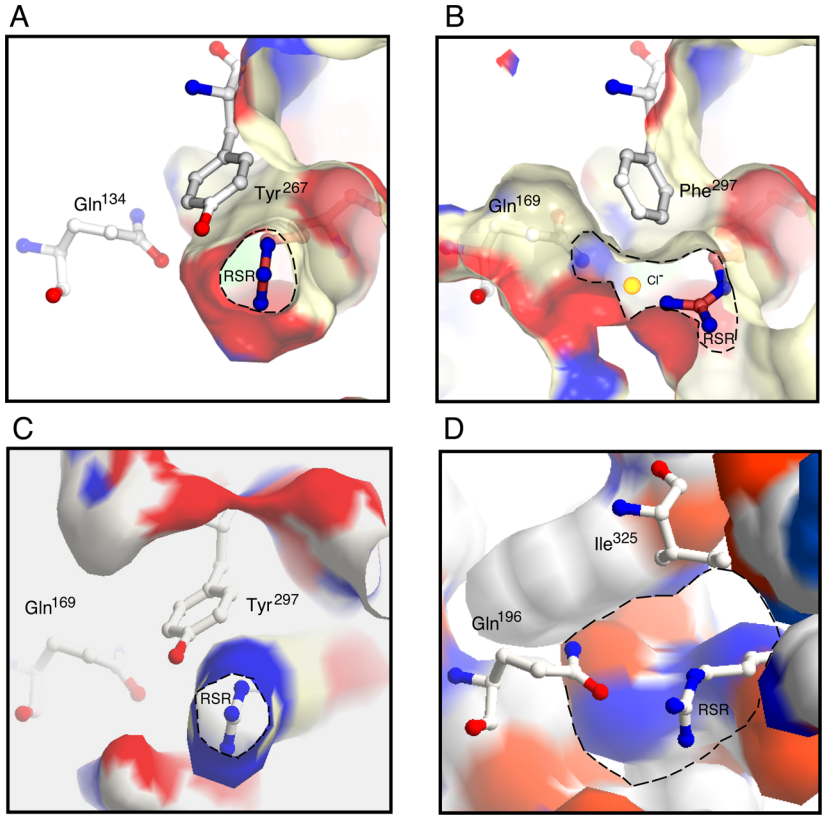

Figure 6. Molecular modeling of the substrate pocket of the wild-type and F297Y APBs. The framework of the S1′ sites coupled with Arg1 of RSR is shown by electrostatic potential (red for negative and blue for positive): (A) LTA4H, (B) APB, (C) F297Y APB, and (D) RNPEP-L1.

peptide substrates may be flexible enough in their orientation to interact with Gln169. In contrast, the narrow pocket of F297Y APB may restrict the proper orientation of the N-terminal basic amino acids of the peptide substrates. Taken together, it is likely that Phe297 plays a critical role in the construction of the optimal substrate pocket required for the APB to exert its characteristic catalytic features.

Several studies of the catalytic mechanism of M1 aminopeptidases have demonstrated the roles of conserved amino acid residues in the exopeptidase motif, GXMEN.[19] It was reported that Glu352 and Asn353 in the motif play roles in the exopeptidase specificity of murine APA through interaction with the N-terminal amino acid of a substrate.[20−23] The conserved Glu within the GXMEN motif has been shown to be involved in the recognition of the α-amino group of the substrates.[21] Gly in the GXMEN motif also contributes to the enzymatic activity and substrate specificity of M1 aminopeptidases such as APB[9] and laeverin/APQ.[17] Recent crystallization of insulin-regulated aminopeptidase (IRAP)/placental leucine aminopeptidase (P-LAP) has revealed that the GXMEN loop adopted a conformation different from that found in other M1 aminopeptidases, explaining its unique specificity for oxytocin and vasopressin.[24] Because Phe297 of APB is located just adjacent to the N-terminal side of the GXMEN motif, it is reasonable to speculate that this residue may be involved in the formation of the optimal global structure necessary for the enzyme to exert its unique catalytic activity.

Figure 7 shows the schematic model of the substrate pocket of APB showing the spatial relationship between several functional amino acid residues and the N-terminal Arg of a

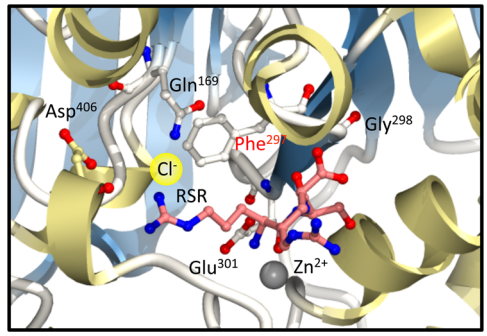

Figure 7. Schematic representation of the substrate pocket of human APB coupled with the putative substrate RSR.

putative peptide substrate RSR. As seen in the figure, Glu301 in the GXMEN motif interacts with the N-terminal amino group of RSR to form the transition complex.[20,21] Because of the space created by Phe297, Gln169 can form a chloride anion-mediated interaction with the amino group of Arg1 of the peptide substrate. It has been reported that like Phe297, Gly298 in the GXMEN motif affects the enzymatic activity and chloride anion sensitivity of APB.[9] However, it seems unlikely that Gly298 can directly affect the formation of the chloride anion bridge. It is plausible that Gly298 facilitates the formation of the appropriate structure of the substrate pocket by supporting the proper positioning of Phe297. Asp406 also interacts with the amino group of the Arg1 side chain, affecting the substrate specificity of the enzyme.[11] Taken together, the data presented in this study suggest that Phe297 contributes to the optimal enzymatic activity of APB via formation and maintenance of the

DOI: 10.1021/acs.biochem.5b00964
Biochemistry 2015, 54, 6062−6070

catalytic pocket, which is wide enough to retain a chloride anion.

It should be mentioned here that the peptidase but not the epoxide hydrolase activity of LTA4H was augmented in the presence of chloride anion.[25] In the analysis of crystal structure of LTA4H, a chloride anion was not observed in the substrate pocket.[18] It is possible that chloride anion affects the aminopeptidase activity of LTA4H via interaction with the enzyme outside of the substrate pocket (see Protein Data Bank entry 3U9W). Alternatively, the substrate pocket of the enzyme might increase in size when an appropriate substrate enters the pocket, allowing chloride anion bridging in the substrate pocket.

In summary, we have shown by site-directed mutagenesis that Phe297 of human APB is important for the maximal enzymatic activity and chloride anion sensitivity of the enzyme. Our molecular modeling suggests that this residue is critical for the formation of the optimal structure of the substrate pocket of the enzyme. X-ray structural analysis of APB is required to elucidate in detail its characteristic catalytic action and how this differs from that of other M1 aminopeptidases.

AUTHOR INFORMATION

Corresponding Author

*Phone: +81-3-5860-4250. Fax: +81-3-5860-4945. E-mail: a.ohnishi@thu.ac.jp.

Funding

This work was supported by a Grant-in-Aid from the Ministry of Education, Culture, Sports, Science and Technology of Japan (Projects 24659153 and 25293083).

Notes

The authors declare no competing financial interest.

ABBREVIATIONS

APB, aminopeptidase B; ERAP, endoplasmic reticulum aminopeptidase; LTA4H, leukotriene A_4 hydrolase; SD, standard deviation.

REFERENCES

(1) Cadel, S., Piesse, C., Pham, V.-L., Pernier, J., Hanquez, C., Gouzy-Darmon, C., and Foulon, T. (2013) Aminopeptidase B. In *Handbook of Proteolytic Enzymes* (Rawlings, N. D., and Salvesen, G. S., Eds.) 3rd ed., pp 473−479, Academic Press, London.

(2) Cadel, S., Pierotti, A. R., Foulon, T., Creminon, C., Barre, N., Segretain, D., and Cohen, P. (1995) Aminopeptidase-B in the rat testes: isolation, functional properties and cellular localization in seminiferous tubules. *Mol. Cell. Endocrinol. 110*, 149−160.

(3) Fukasawa, K. M., Fukasawa, K., Kanai, M., Fujii, S., and Harada, M. (1996) Molecular cloning and expression of rat aminopeptidase B. *J. Biol. Chem. 271*, 30731−30735.

(4) Tsujimoto, M., and Hattori, A. (2005) The oxytocinase subfamily of M1 aminopeptidases. *Biochim. Biophys. Acta, Proteins Proteomics 1751*, 9−18.

(5) Hwang, S.-R., O'Neill, A., Bark, S., Foulon, T., and Hook, V. (2007) Secretary vesicle aminopeptidase B related to neuropeptide processing: molecular identification and subcellular localization to enkephalin- and NPY-containing chromaffin granules. *J. Neurochem. 100*, 1340−1350.

(6) Fontes, G., Lajoix, A.-D., Bergeron, F., Cadel, S., Prat, A., Foulon, T., Gross, R., Dalle, S., Le-Nguyen, D., Tribillac, F., and Bataille, D. (2005) Miniglucagon (MG)-generating endopeptidase, which processes glucagon into MG, is composed of N-arginine dibasic convertase and aminnopeptidase B. *Endocrinology 146*, 702−712.

(7) Beinfeld, M., Funkelstein, L., Foulon, F., Cadel, S., Kitagawa, K., Toneff, T., Reinheckel, T., Peters, C., and Hook, V. (2009) Cathepsin L plays major role in cholecystokinin production in mouse brain cortex in pituitary AtT-20 cells: protease gene knockout and inhibitor studies. *Peptides 30*, 1882−1891.

(8) Pham, V.-L., Cadel, M.-S., Gouzy-Darmon, C., Hanquez, C., Beinfeld, M. C., Nicolas, P., Etchebest, C., and Foulon, T. (2007) Aminopeptidase B, a glucagon-processing enzyme: site directed mutagenesis of the Zn^{2+}-binding motif and molecular modeling. *BMC Biochem. 8*, 21.

(9) Pham, V.-L., Gouzy-Darmon, C., Pernier, J., Hanquez, C., Hook, V., Beinfeld, M. C., Nicolas, P., Etchebest, C., Foulon, T., and Cadel, S. (2011) Mutation in the substrate-binding site of aminopeptidase B confers new enzymatic properties. *Biochimie 93*, 730−741.

(10) Cadel, S., Darmon, C., Pernier, J., Hervé, G., and Foulon, T. (2015) The M1 family of vertebrate aminopeptidases: role of evolutionarily conserved tyrosines in the enzymatic mechanism of aminopeptidase B. *Biochimie 109*, 67−77.

(11) Fukasawa, K. M., Hirose, J., Hata, T., and Ono, Y. (2006) Aspartic acid 405 contributes to the substrate specificity of aminopeptidase B. *Biochemistry 45*, 11425−11431.

(12) Ogawa, Y., Ohnishi, A., Goto, Y., Sakuma, Y., Watanabe, J., Hattori, A., and Tsujimoto, M. (2014) Role of glutamine-169 in the substrate recognition of human aminopeptidase B. *Biochim. Biophys. Acta, Gen. Subj. 1840*, 1872−1881.

(13) Diaz-Perales, A., Quesada, V., Sanchez, L. M., Ugalde, A. P., Suarez, M. F., Fueyo, A., and Lopez-Otin, C. (2005) Identification of human aminopeptidase O, a novel metallopeptidase with structural similarity to aminopeptidase B and leukotriene A_4 hydrolase. *J. Biol. Chem. 280*, 14310−14317.

(14) Maruyama, M., Hattori, A., Goto, Y., Ueda, M., Maeda, M., Fujiwara, H., and Tsujimoto, M. (2007) Laeverin/aminopeptidase Q, a novel bestatin-sensitive leucine aminopeptidase belonging to the M1 family of aminopeptidases. *J. Biol. Chem. 282*, 20088−20096.

(15) Fukasawa, K. M., Fukasawa, K., Harada, M., Hirose, J., Izumi, T., and Shimizu, T. (1999) Aminopeptidase B is structurally related to leukotriene-A_4 hydrolase but is not a bifunctional enzyme with epoxide hydrolase activity. *Biochem. J. 339*, 497−502.

(16) Thompson, M. W., Beasley, K. A., Schmidt, M. D., and Seipelt, R. L. (2009) Arginyl aminopeptidase-like 1 (RNPEPL1) is an alternatively processed aminopeptidase with specificity for methionine, glutamine, and citrulline residues. *Protein Pept. Lett. 16*, 1256−1266.

(17) Maruyama, M., Arisaka, N., Goto, Y., Ohsawa, Y., Inoue, H., Fujiwara, H., Hattori, A., and Tsujimoto, M. (2009) Histidine 379 of human laeverin/aminopeptidase Q, a nonconserved residue within the exopeptidase motif, defines its distinctive enzymatic properties. *J. Biol. Chem. 284*, 34692−34702.

(18) Thunnissen, M. M., Nordlund, P., and Haeggstrom, J. Z. (2001) Crystal structure of human leukotriene A_4 hydrolase, a bifunctional enzyme in inflammation. *Nat. Struct. Biol. 8*, 131−135.

(19) Tsujimoto, M., Goto, Y., Maruyama, M., and Hattori, A. (2008) Biochemical and enzymatic properties of the M1 family of aminopeptidases involved in the regulation of blood pressure. *Heart Failure Rev. 13*, 285−291.

(20) Vazeux, G., Iturrioz, X., Corvol, P., and Llorens-Cortes, C. (1998) A glutamate residue contributes to the exopeptidase specificity in aminopeptidase A. *Biochem. J. 334*, 407−413.

(21) Luciani, N., Marie-Claire, C., Ruffet, E., Beaumont, A., Roques, B. P., and Fournie-Zaluski, M. C. (1998) Characterization of Glu350 as a critical residue involved in the N-terminal amine binding site of aminopeptidase N (EC 3.4.11.2): insights into its mechanism of action. *Biochemistry 37*, 686−692.

(22) Rudberg, P. C., Tholander, F., Thunnissen, M. M., and Haeggstrom, J. Z. (2002) Leukotriene A_4 hydrolase/aminopeptidase; glutamine 271 is a catalytic residue with specific roles in two distinct enzyme mechanisms. *J. Biol. Chem. 277*, 1398−1404.

(23) Iturrioz, X., Rozenfeld, R., Michaud, R., Corvol, P., and Llorens-Cortes, C. (2001) Study of asparagine 353 in aminopeptidase A: characterization of movel motif (GXMEN) implicated in exopeptidase

DOI: 10.1021/acs.biochem.5b00964
Biochemistry 2015, 54, 6062−6070

specificity of monozinc aminopeptidases. *Biochemistry 40*, 14440−14448.
(24) Hermans, S. J., Ascher, D. B., Hancock, N. C., Holien, J. K., Michell, B. J., Chai, S. Y., Morton, C., and Parker, M. W. (2015) Crystal structure of human insulin-regulated aminopeptidase with specificity for cyclic peptides. *Protein Sci. 24*, 190−199.
(25) Wetterholm, A., and Haeggstrom, J. Z. (1992) Leukotriene A4 hydrolase: an anion activated peptidase. *Biochim. Biophys. Acta, Lipids Lipid Metab. 1123*, 275−281.

DOI: 10.1021/acs.biochem.5b00964
Biochemistry 2015, 54, 6062−6070